Journal of Molecular Structure 1349 (2026) 143720

Contents lists available at ScienceDirect

Journal of Molecular Structure

journal homepage: www.elsevier.com/locate/molstr

Novel structure motif for the selective inhibition of TET1 protein based on perimidines

Zdeněk Kejík [a,b], Robert Kaplánek [a,b], Nikita Abramenko [a,b], Frédéric Vellieux [a,b], Kateřina Veselá [a,b], Petr Babula [e], Michal Masařík [a,d,e], Jan Ulrich [c], Kateřina Kučnirová [a,b], Jan Hajduch [a], Pavel Martásek [b,*], Milan Jakubek [a,b,*]

[a] BIOCEV, First Faculty of Medicine, Charles University, Průmyslová 595, 252 50 Vestec, Czech Republic
[b] Department of Paediatrics and Inherited Metabolic Disorders, First Faculty of Medicine, Charles University and General University Hospital in Prague, Ke Karlovu 455/2, 128 08 Prague, Czech Republic
[c] Department of Surgery-Department of Abdominal, Thoracic Surgery and Traumatology, First Faculty of Medicine, Charles University and General University Hospital, U Nemocnice 2, 121 08 Prague, Czech Republic
[d] Department of Pathological Physiology, Faculty of Medicine, Masaryk University, Kamenice 5, 625 00 Brno, Czech Republic
[e] Department of Physiology, Faculty of Medicine, Masaryk University, Kamenice 5, 625 00 Brno, Czech Republic

ARTICLE INFO

Keywords:
TET proteins
Inhibitors
Iron chelators
Perimidine
Molecular docking

ABSTRACT

The targeting of epigenetic factors, particularly TET proteins (ten-eleven translocation methylcytosine dioxygenases), has emerged as a significant focus in medicinal and biological research. Recent findings indicate that iron chelators possess substantial potential for inhibiting TET activity. In this study, we synthesized two 2-(hetero)aryl-1H-perimidines (perimidine **1** and **2**) with iron(II) binding properties. The results show that these derivatives, particularly **2**, exhibit notable inhibitory activity and selectivity for the TET1 protein, with an IC_{50} value of 1.02 μM, in contrast to TET2, which has an IC_{50} value of 13.23 μM.

Regulation of gene expression is one of the most important regulatory mechanisms in living systems [1]. Epigenetic regulations, such as DNA modifications, play a significant role in this process [2]. 5-methylcytosine and 5- hydroxymethylcytosine (5mC and 5hmC; called as the fifth and sixth base of DNA, respectively) play key roles in the regulation of gene expression. In gene promoters (CpG islands), 5mC supports gene silencing, whereas 5hmC is more associated with gene expression [3–6]. In living systems, the balance between 5mC and 5hmC is controlled by ten-eleven translocation proteins (TETs) [7,8]. TET proteins are Fe(II) and α-ketoglutarate-dependent dioxygenases that gradually oxidise 5mC to 5hmC. Therefore, dysregulation of TET protein activity can have serious health implications. For example, increased activity of TET1 is associated with the development and progression of MLL-rearranged leukaemia, non-small-cell lung carcinoma, and triple-negative breast cancer [9–11]. Additionally, several findings imply its significant role in the pathogenesis of autoimmune and neurodegenerative diseases [12].

Currently, inhibitors of TET proteins are being developed as potential new therapeutics [13–15]. Notably, the catalytic domain of the TET1 protein exhibits a high degree of similarity with the catalytic domain of other TET proteins, particularly TET2. However, there are significant differences in the protein regions responsible for interactions with DNA and with other proteins [16]. Consequently, their functionalities diverge, making effective targeting a considerable challenge. In this context, cyclic peptide inhibitors with potent selectivity for the TET1 protein have been reported [17,18]. On the other hand, small molecule inhibitors may offer superior pharmacokinetic properties compared to peptides [19]. Consequently, there is currently an urgent need for selective small molecular inhibitors of TET proteins.

In medicinal chemistry, very promising results have often been reported for compounds containing N-composed heterocyclic motifs. These compounds feature a double bond between a nitrogen atom and a carbon atom (−C=N−) in combination with substituents, usually alkyl or aryl groups [20–26]. They possess numerous intriguing properties such as high and selective inhibition of enzyme activity (e.g., urease, carbonic anhydrase, α-amylase, α-glucosidase, and prolyl oligopeptidase), and they can act as ligands for transition metal ions.

Because of the presence of the Fe(II) ion in the active site of TET proteins, iron chelators are one possible type of developed inhibitors

* Corresponding authors.
E-mail addresses: zkejik@centrum.cz (Z. Kejík), Pavel.Martasek@lf1.cuni.cz (P. Martásek), Milan.Jakubek@lf1.cuni.cz (M. Jakubek).

https://doi.org/10.1016/j.molstruc.2025.143720
Received 21 July 2025; Received in revised form 14 August 2025; Accepted 20 August 2025
Available online 20 August 2025

[27–30]. Perimidines (tricyclic heterocycles with a monohydropyrimidine ring ortho- and peri-fused to a naphthalene scaffold) [31] and their derivatives have long been used as receptors for divalent metal ions [32,33]. Unfortunately, our knowledge regarding their interactions with Fe(II) ions is quite limited. Nevertheless, it is well recognised that the structural motif of Fe(II) chelators is often characterized by the presence of nitrogen heteroaromatic groups [34,35]. This suggests that perimidines may serve as promising building blocks in the design of Fe(II) chelators. Additionally, perimidines represent an intriguing structural motif in the development of therapeutics (e.g., anticancer agents), [31] including enzyme inhibitors [36].

The above raises the question of whether the pyrimidine structural motif could also be utilised in the design of TET protein inhibitors. Its combination with other suitable groups to target TET proteins could lead to the development of potent TET inhibitors. Our previous results suggest that the hydroxyphenyl group is a promising candidate for targeting TET proteins [28,30,37]. On the other hand, nitrogen-containing heterocycles could mimic the interaction of DNA bases with TETs [38]. In the present study, we therefore designed, synthesised, and studied perimidine derivatives containing substituted 2-hydroxyphenyl or 2-pyridine groups as a novel class of Fe(II) chelators and potential TET1 protein inhibitors.

1. Results

1.1. Chemistry

Perimidines **1** and **2** were prepared by the reaction of equimolar amounts of naphthalene-1,8-diamine with 2-hydroxy-3-methoxybenzaldehyde and 3-methylpyridine-2-carbaldehyde, respectively, in the presence of a threefold excess of sodium pyrosulfite as an oxidant at 70 °C in ethanol (Scheme 1) [33]. The progress of the reactions was thoroughly examined by means of thin-layer chromatography using dichloromethane-methanol (10:1, v/v) or diethyl ether as a solvent system. After evaporation to dryness, the crude products were purified by column chromatography on silica gel (eluent: dichloromethane-methanol 10:1 v/v). ^{1}H and ^{13}C NMR spectroscopy was performed to confirm the structures of perimidines **1** and **2**. Characteristic signals include singlets at δ 3.80 ppm for the methoxy group of **1** and δ 2.64 ppm for the methyl group of **2**, respectively. Signals in the downfield region of the spectrum at δ 10.66 and 10.61, respectively, were due to perimidine NH protons. The determined values of molecular masses of perimidines **1** and **2** (291.2 and 260.0) were consistent with the calculated values (291.1 and 260.1, respectively).

1.2. In silico docking of perimidines *1* and *2* to the TET1 and TET2 models

For docking calculations, we used a structural model of the catalytic domain of TET1 (obtained by homology modelling using a method essentially identical to that published by Chua *et al.*, 2019, starting from the 3D structure of TET2 (PDB id 4NM6) [39]. *In silico* mutations (from the amino acid sequence of TET2 to TET1 sequence) were introduced using the Coot program [40]. This step used the published sequence alignment given in Chua et al. [39] The resulting TET1 model contains the polypeptide chain and Fe(II) ion in the catalytic domain. To prepare the TET2 protein model, we used a high-resolution crystallographic structure (PDB id 5DEU) [41].

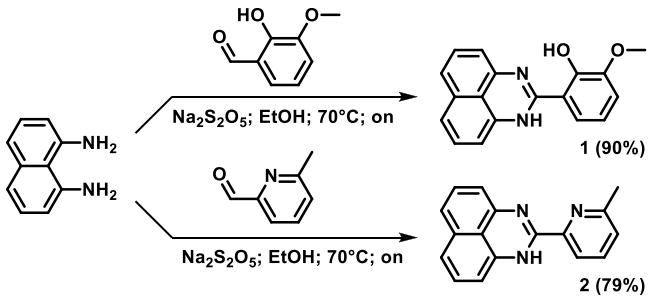

Scheme 1. Preparation of perimidines **1** and **2.**

The structures of the ligands used in our study, perimidines **1** and **2**, were drawn using ChemDraw software [29]. Our calculations showed that in both cases — before and after equilibration — perimidine **2** exhibited a higher binding energy than perimidine **1**. The values of binding energy are shown in Table 1. In this section, we will therefore focus only on the more promising compound – perimidine **2** (Fig. 1 and 2).

The 2D diagram shows that Fe(II) in the catalytic site of TET1 forms *π-anion* interactions with perimidine **2**, with a slightly shorter distance (3.4 Å) compared to perimidine **1** (3.6 Å) (Fig. 3, **S1 and S2**). Additionally, one of key interactions is the *π-sulphur* interaction between CYS 1263 and the ligand. Again, we observe a slightly shorter distance for this interaction in the case of perimidine **2** (5.1 Å) compared to value of 5.5 Å for perimidine **1**.

Further, we observe other non-covalent interactions. A *π-Cation* interaction occurs between the positively charged side chain of ARG 1261 and the aromatic system of perimidine **2** (orange dashed lines). *π-anion* interactions are observed in ASP 1384 (purple lines), where the negatively charged carboxyl group interacts with the ligand's aromatic ring. *π–π stacking* and *T-shaped* interactions (pink dashed lines) are observed with TYR 1532, HIS 1382, and other residues, stabilizing the ligand through aromatic π-π interactions. *Alkyl* and *π-alkyl* contacts (pink) are observed with VAL 1395, VAL 1530, PHE 1377, ALA 1379, and CYS 1374, contributing additional weak hydrophobic interactions. Finally, *van der Waals* interactions (green) with residues such as ASN 1387, HIS 1386, HIS 1534, and HIS 1511 help stabilize the ligand within the binding site.

A comparison of the binding modes is shown in Figs. 3, **S1 and S2**. Across all four binding scenarios (TET1@**1**, TET2@**1**, TET1@**2**, and TET2@**2**), ligand stabilization is primarily governed by *van der Waals* forces, emphasizing the role of shape complementarity within the active sites. In the case of TET1, we can observe a pattern that includes *π-anion* interactions with Fe(II) ion. Fe(II) is a positively charged metal ion that typically forms *π-cation* interactions with electron-rich aromatic systems (such as the side chains of TYR or TRP). However, in the case of TET1, the interaction between Fe(II) and the ligands perimidine **2** and perimidine **1** is classified as a *π-anion* interaction rather than a *π-cation* one [42]. In metalloenzymes like TET1, Fe(II) is not freely exposed but is coordinated within the active site by surrounding residues (such as HIS, ASP, or CYS). This coordination modifies the electronic environment around Fe(II), often making it less electrostatically positive than a free Fe(II) ions in solution, especially when Fe(II) is surrounded by negatively charged residues (e.g., ASP or GLU). A partial redistribution of electron density may occur, which in this context leads to behavior similar to that of electron-rich species [43,44].

Also the analysis of interactions of the TET1 complex with perimidines **1** and **2** revealed considered interaction modes involving key residues that contribute to ligand stabilization. Notably, CYS 1263, ASP 1384, and HIS 1382 interact with the pyrimidine region of the ligand through distinct non-covalent interactions, forming a stable binding network. CYS 1263 participates in a *π-sulfur* interaction, where its sulfur

Table 1
Computed value of binding energy between perimidines 1 and 2 and proteins TET1 and TET2 (after an equilibration step).

Compound	Binding energy /[kcal/mol]	
	TET1	TET2
perimidine **1**	−8.4	−6.589
perimidine **2**	−9.186	−9.306

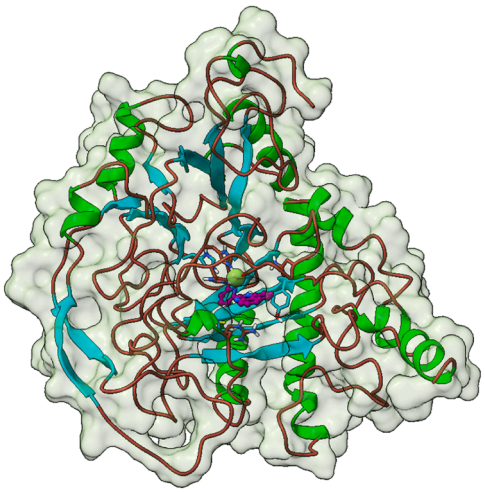

Fig. 1. A general view of perimidine 2 (violet) positioning of the TET1 active site (−9.186 kcal/mol).

atom interacts with the π-system of the ligand. ASP 1384 establishes *π-anion* interactions, where its negatively charged carboxylate group (-COO⁻) interacts with the electron-deficient π-system of the ligand. This interaction strengthens the ligand binding by providing additional electrostatic stabilization. HIS 1382 contributes through a *π-cation* interaction, where its positively charged imidazole ring interacts with the ligand's electron-rich *π*-system. Such interactions are commonly observed in metal-dependent enzymes and may facilitate ligand orientation near Fe(II) within the active site [45–47]. We can also observe an aromatic type of interaction with TYR 1532. TYR 1532 contributes to ligand stabilization through *π-π T-shaped* interactions, reinforcing the hydrophobic and electrostatic network that governs ligand binding in TET1 [48].

The pyridine region of perimidine **2** bond to TET1 consistently interacts with a group of amino acid residues, including HIS 1416, ALA 1379, VAL 1395, CYS 1374, and VAL 1530, which engage in *alkyl* and *π-alkyl* interactions, reinforcing the hydrophobic pocket that accommodates the ligand.

The binding interactions of the perimidines **1** and **2** within the active site of TET2 exhibit distinct patterns compared to TET1. The key residues contributing to ligand stabilization in TET2 include ARG 1262, ARG 1261, ASP 1384, GLU 1267 and CYS 1374, which bind to ligands via *convential, carbon* and *π-donor hydrogen bonds.* ARG 1262 forms a conventional hydrogen bond with the hydroxyl group of the methoxy-catechol moiety of perimidine **1**, while GLU 1267 forms a carbon hydrogen bond with the methyl group of the methoxy-catechol moiety of perimidine **1**. Also ARG 1262 forms *π-alkyl* interactions with the pyrimidine moiety of perimidine **1**, while HIS 1380 interacts with the methyl group of the methoxy-catechol moiety of perimidine **1** via *a π-alkyl* bond. Additionally, LEU 1385 forms a *π-sigma* interaction with one of the aromatic rings of the pyrimidine moiety.

ARG 1261 and ASP 1384 form conventional hydrogen bonds with the pyrimidine moiety of the perimidine **2**, while CYS 1374 forms a π-donor hydrogen bond. Additionally, ARG 1261 engages in a π-cation interaction with the pyridine group of perimidine **2**. HIS 1382 forms π-π T-shaped interactions with the pyrimidine moiety of perimidine **2**, while TYR 1533 forms π-π stacked and π-alkyl interactions with the pyridine moitey of perimidine derivatives **2**. Additionally, VAL 1531 forms a π-sigma interaction with the pyrimidine ring. The presence of van der Waals interactions with residues like ALA 1379, THR 1372, and SER 1284 suggests a hydrophobic environment that helps in ligand accommodation and retention.

Binding Study of Compounds with Fe(II) ions

For used iron chelators, the presumed mechanism of inhibition is associated with the interaction of the Fe(II) ion at the active site of the enzyme. The chelation ability of the prepared compounds in aqueous surroundings was investigated using UV–VIS spectroscopy (Fig. **S3** and **4**). Their interaction with Fe(II) ions was associated with a strong spectral response. For example, in the case of perimidine **2**, a gradual decrease in absorption was observed at 282 nm, 334 nm, and 345 nm when the concentration of added ions increased from 0 to 0.25 equivalents (Figure). Nevertheless, the addition of Fe(II) ion (from 0 to 0.2 equivalents) also led to an increase in absorption at a new maximum (at 373 nm). It can be suggested that perimidine **2** can form two types of complexes with Fe(II) ion in aqueous surroundings (1:4 and 1:5; Fe(II): chelator).

Both tested chelators exhibited a significant affinity for iron ions (Table 2). However, a significantly higher affinity was observed for perimidine **2**, suggesting that the pyridine group, in combination with pyrimidine, represents a more effective structural motif for Fe(II) chelation compared to ortho-hydroxy methoxyphenyl.

Inhibition of TET1 and TET2 protein using perimidines 1 and 2

The effects of perimidines **1** and **2**inhibitors on the activity of TET1 and TET2 were assessed using Bioscience chemiluminescence kits (TET1: 50651, TET2: 50652). The enzymes TET1 and TET2 were included as part of the mentioned kits, respectively. This approach was also used by Chua et al. [39] Both tested compounds demonstrated

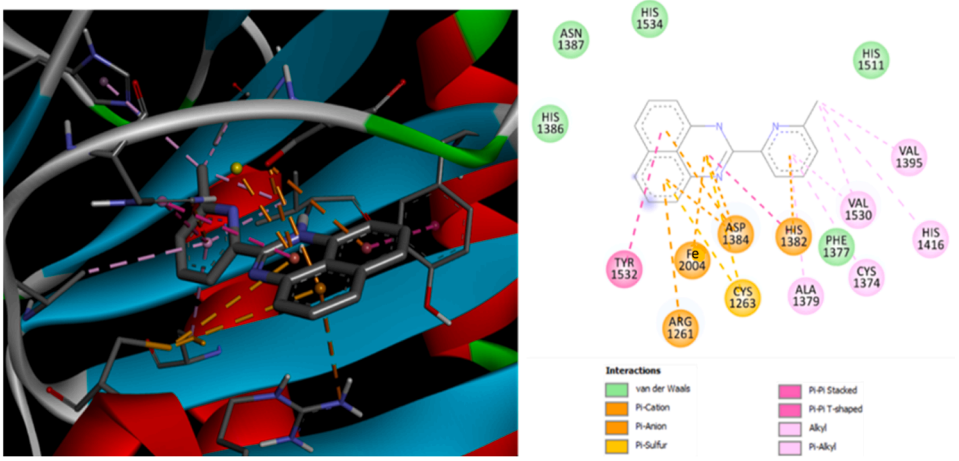

Fig. 2. Binding interactions between perimidine **2** and protein TET1. The left panel presents a 3D visualization of the molecular docking results, highlighting the position of the ligand within the active site of TET1. The right panel displays a 2D interaction diagram, where various types of non-covalent interactions between perimidine **2** and key amino acid residues of the protein are indicated using different colours and line styles.

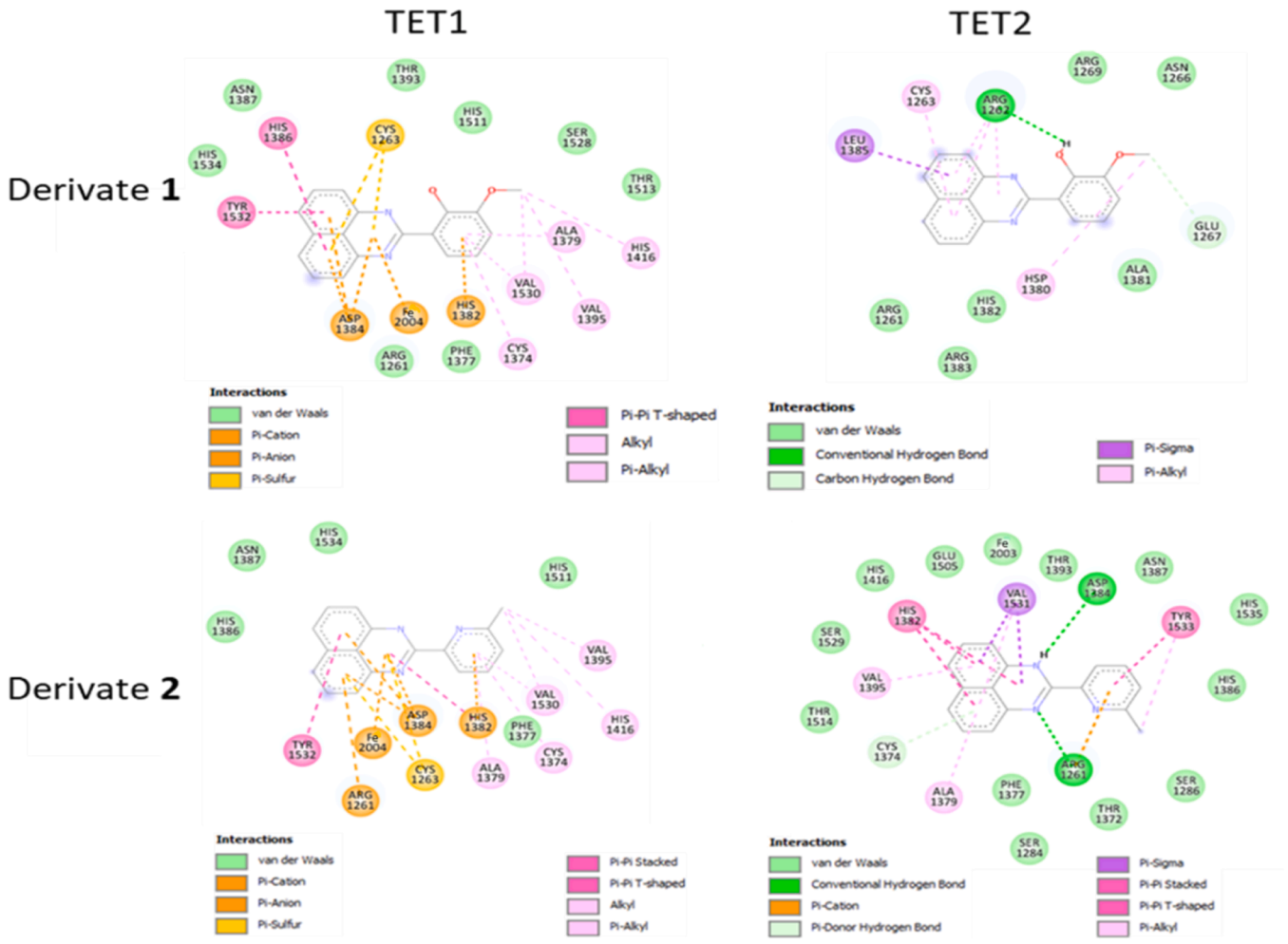

Fig. 3. Comparison of binding modes of TET1 and TET2 with perimidines **1** and **2**.

Table 2
Conditional binding constants and complex stoichiometry of chelator complexes with Fe(II) ion.

Chelator	Log (K)	Stoichiometry (metal: chelator)
perimidine **1**	11.029±0.59	1:2
perimidine **2**	23.81±0.51	1:4
	29.023±0.78	1:5

Table 3
Influence of chelators on the activity of TET1 and TET2 protein.

Chelators	TET1 protein		TET2 protein		Selectivity
	IC_{50} /μM	Chelated Fe (II)[a] %	IC_{50} /μM	Chelated Fe (II) %	
perimidine **1**	1.43	0.59	5.41	2.25	3.78
perimidine **2**	1.02	0.42	13.5	5.62	13.23
Deferoxamine	>450	~100	>450	~100	–

a The value expresses the potential reduction of free Fe(II) concentration through a chelation effect. The considered concentrations of perimidine **1** and **2,** as well as deferoxamine, correspond to their IC_{50} values for the respective TET proteins. The expected complex stoichiometry is 1:2 for the prepared chelators and 1:1 for deferoxamine (Fe(II)). It is assumed that all chelators participate in the complexation.

potent Fe(II) chelation properties, and their potential inhibitory effects could also stem from a significant reduction in the levels of free Fe(II) ions rather than direct interaction with the enzyme. A Fe(II) ion concentration of 0.12 mM was used in the TET1 protein kit, while only 0.004 mM was used for the TET2 protein. Given the expected IC_{50} value (micromolar), it can be concluded that the Fe(II) concentration for TET2 protein was too low and that the tested concentrations could have led to a significant depletion of Fe(II) ions, thereby inhibiting enzyme activity. Consequently, the Fe(II) concentration was increased to 0.12 mM. Additionally, to improve the discrimination of the chelation effect, a potent Fe chelator (deferoxamine) was utilized as a control at the same concentration as the prepared chelators. Both perimidines **1** and **2**, displayed comparable inhibitory effects on TET1 protein (Figure and Figure , Fig. **S4** and **S3**, Table 3**, S1** and **S2**).

However, in the case of TET2, the inhibitory effect of perimidine **1** was significantly greater than that of **2** (Fig. 4, 5, 6). Notably, both chelators, particularly perimidine **2**, exhibited several times higher inhibitory effects on TET1, with an IC_{50} of 1.023 μM, compared to TET2, which had an IC_{50} of 13.53 μM. The obtained IC_{50} values strongly suggest that the mechanism of inhibition by the tested chelators is not merely dependent on the nonselective complexation of free Fe(II) in medium. For example, the concentration of the tested chelators that led to a 50 % reduction in enzyme activity did not result in a significant decrease in the concentration of free Fe(II) ions. In the case of deferoxamine, the inhibitory effects remained significant, but the obtained results indicated that the IC_{50} values were higher than 450 μM. In the reflex stoichiometry of the complex (1:1), [49] the decrease in the level of free Fe(II) is than comparable with decrease enzymes activity.

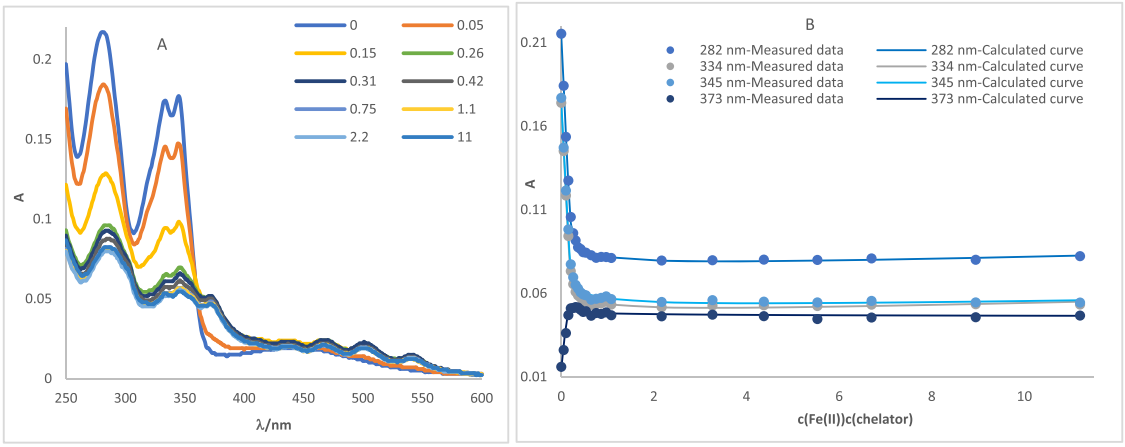

Fig. 4. UV–Vis spectra of perimidine **2** in the presence of Fe(II) ions (A) and titration curve (B) for perimidine **2** (10 μM) showing the dependence of the complex absorbance on the Fe(II) concentration in aqueous medium (water/DMSO, 99:1, v/v).

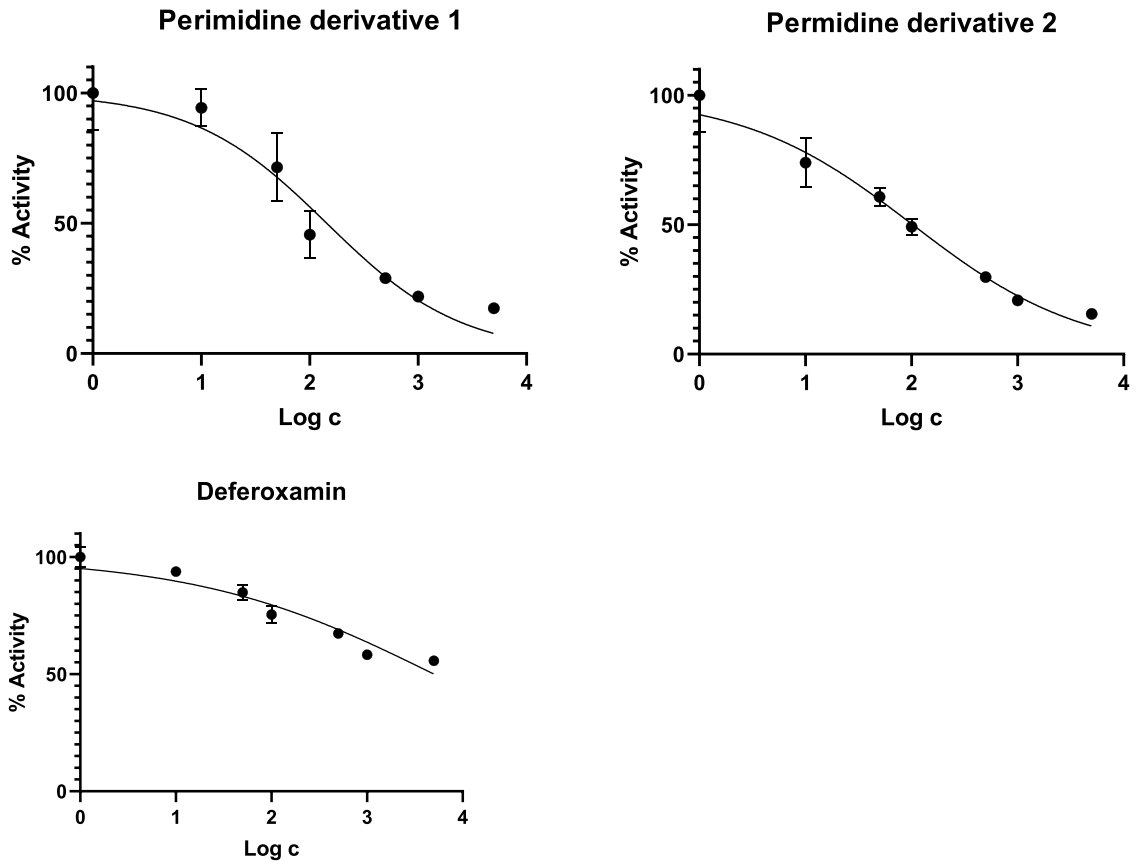

Fig. 5. Dose-response curve of residual TET1 activity on the concentration of tested chelators (perimidines **1** and **2** and deferoxamine).

2. Discussion

In silico docking studies suggest that perimidine **1** could exhibit significantly higher affinity and inhibition activity for TET1 protein compared to TET2. This finding was further corroborated by experimentally obtained IC_{50} values. However, in the case of perimidine **2**, the interaction energy value suggests that this chelator may have comparable affinity for both TET1 and TET2 proteins. Notably, the IC_{50} for the perimidine **2** with TET2 was an order of magnitude higher, which can be attributed to the lack of a direct correlation between IC_{50} values and binding energy [50]. It is important to note that molecular docking of TET1 was performed on a homologous model based on the structure of TET2, whereas docking of TET2 was conducted on its experimentally determined crystal structure.

The obtained results imply that perimidines **1** and **2** can target critical parts in the active sites of TET1 and TET2 proteins, such as ARG 1261. ARG 1261 participates in substrate binding via a water-mediated hydrogen bond between the hydrofuran oxygen (from deoxyribose DNA) and α-ketoglutarate (the co-factor of TET proteins) [38]. Additionally, perimidines also bind Fe(II), except for the interaction of perimidine **1** with TET2. The Fe(II) ion in the active site plays a key role in the oxidation of the cytosine group in 5mC.

Furthermore, a significant role in the mechanism of inhibition could also be played by the interaction of perimidines **1** and **2** with the iron

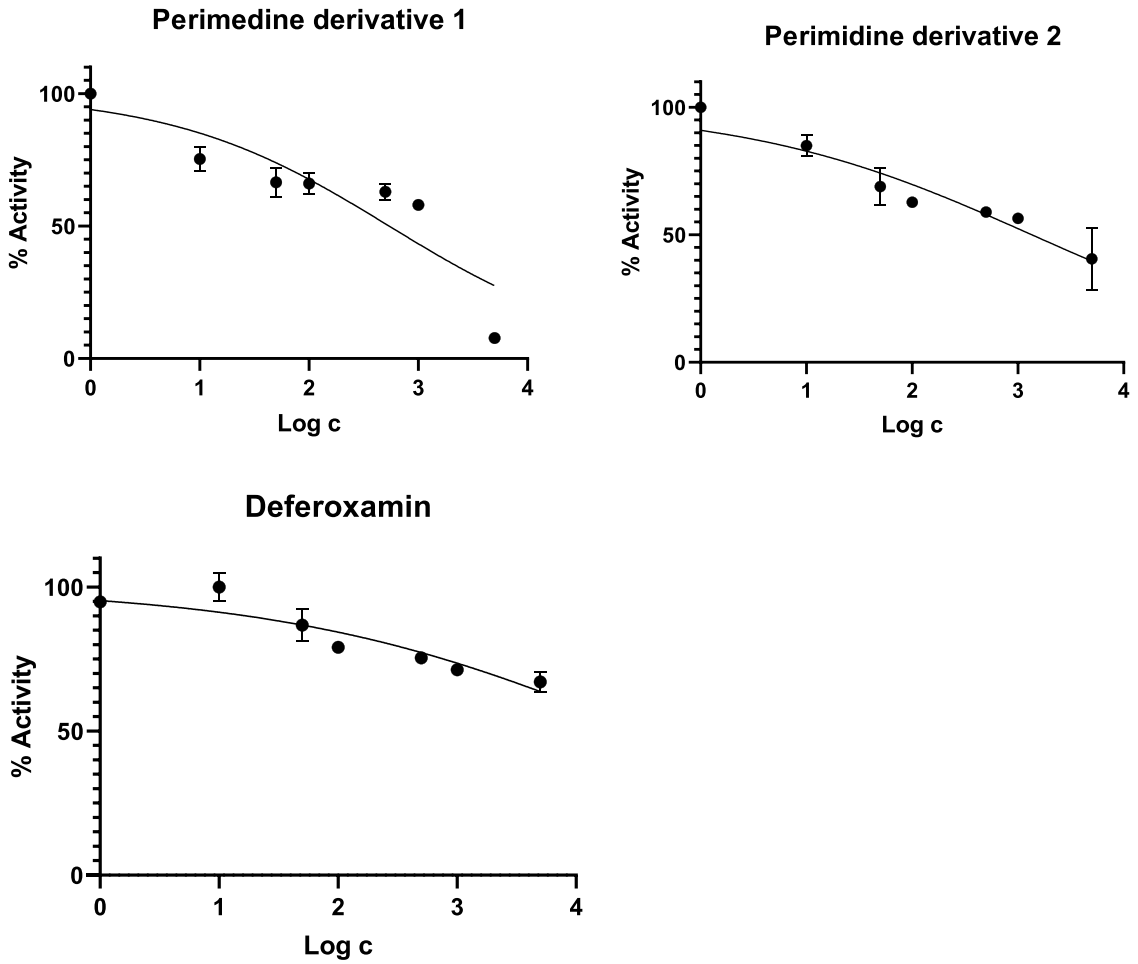

Fig. 6. Dose-response curve of residual TET2 activity on the concentration of tested chelators (perimidines **1** and **2** and deferoxamine).

coordination groups (HIS 1382 and ASP 1384). The HIS 1382/ASP 1382 mutations in the TET2 protein are associated with a significant decrease in enzyme activity [12]. In the case of the TET1 protein, the obtained results imply that perimidines **1** and **2** can interact with both 1382 HIS and 1384 ASP. However, in the case of TET2, perimidines **1** and **2** interact only with 1382 HIS and 1384 ASP, respectively.

In the case of non-substituted perimidine, molecular docking predicts interactions with ARG 1261, the Fe(II) ion, 1382 HIS, and 1384 ASP in the active site of both TET1 and TET2 proteins (Fig. S6). Nevertheless, the computed values of binding energy were approximately 6.4 kcal/mol. This suggests that the perimidine core alone is sufficient for the inhibition of TET proteins, but with lower affinity/inhibition activity and is probably non-selective. This also suggests that the difference in binding energy alone may not be enough to predict selectivity; the importance of targeted residues for the mechanism of enzyme catalysis should also be considered.

Nevertheless, it is obvious that both tested inhibitors, particularly perimidine **2** (with a selectivity greater than 13x), display significant selectivity for the TET1 protein. The majority of the tested low molecular weight inhibitors exhibit comparable inhibition activity against TET protein isoforms [27]. In this context, it is worth mentioning that Guan et al. prepared TETi76, a carboxylic acid derivative that exhibits potent selectivity (~8x) for TET1 compared to TET2 [13]. Interestingly, docking studies suggest a possible interaction between the Fe(II) ion in the active site of TET2 proteins and perimidines **1** and **2**. Analysis of the interaction of perimidine **1** with Fe(II) ions showed the possibility of complex formation with 1:1 stoichiometry, but its K value is very low (Log K = −0.24; Fig. **S7A** and Table **S3**). When analysing the stoichiometry for the binding of perimidine **2** in a 1:1 ratio, the obtained value was significant (Log K = 5.86; Fig. **S7B** and Table **S3**). It is important to note that binding constants can only be accurately calculated using titration curves at specific wavelengths: 282 nm, 334 nm, and 345 nm. Consequently, the titration curve at 373 nm must be excluded from the stoichiometry calculations to prevent cycling errors. This implies that in the case of interaction of perimidines **1** and **2** with the Fe(II) ion in the enzyme's active site occurs, but this interaction is not significantly stronger than others.

As expected, the inhibitory activity of deferoxamine ($IC_{50} > 450$ μM) was observed for both TET1 and TET2. Palei et al. reported a significantly stronger effect of deferoxamine on the activity of the TET2 protein ($IC_{50} = 46$ μM) [51]. However, it is important to note that in this case, a significantly smaller amount of Fe(II) ions was used (75 μM $(NH_4)_2Fe(SO_4)_2$). This suggests that deferoxamine effect is strongly negatively correlated with the concentration of Fe(II) ions. It implies that deferoxamine most likely does not directly interact with TET proteins but rather decreases their activity primarily through the chelation of Fe(II) ions.

Currently, the potential usability of the tested inhibitors may be in question. One possible area for application could be the development of anticancer drugs. For example, the TET protein inhibitor Bobcat339, which has a strong effect against breast cancer cells with high metastatic activity, displays IC_{50} values of 33 and 73 μM for TET1 and TET2, respectively, with the same kit used in this study [39,52]. Its anticancer effects are more strongly associated with the inhibition of TET1 than that of TET2. The prepared compounds, especially perimidine **2**, show high potential in anticancer treatment. It should also be mentioned that

perimidine derivatives display inhibitory activity against topoisomerase II, another DNA-targeting enzyme [36]. On the other hand, pyrimidines are used as building blocks, and knowledge of their biological effects is necessary for the correct evaluation of their toxicity. Additionally, in biological research, selective inhibitors of the TET1 protein, such as perimidine **2**, compared to TET2, could serve as promising tools for studying the role of TET proteins in gene expression.

The above suggests that the tested chelators, especially perimidine **2**, represent promising structure motif for the in design of novel therapeutic agents based on the inhibition of TET1 proteins.

3. Materials and methods

3.1. General comments

All chemicals and solvents were purchased from commercial sources and were used without further purification. NMR spectra were obtained with a Bruker Avance III 500 MHz (500 MHz for 1H and 125 MHz for 13C) (Bruker, Germany) at 25 °C DMSO-d_6. The chemical shifts (δ) are presented in ppm and the coupling constants (*J*) in Hz. Measured NMR spectra are showed on the Figure **S8-S11**. Mass spectra were measured with a 3200 Q TRAP mass spectrometer (AB Sciex, Canada) fitted with an electrospray ion source.

3.2. Preparation of perimidine derivatives

Perimidine **1** (2-(2-hydroxy-3-methoxyphenyl)-1*H*-perimidine)

Naphthalene-1,8-diamine (119 mg; 0.75 mmol), 2-hydroxy-3-methoxybenzaldehyde (114 mg; 0.75 mmol) and sodium pyrosulfite (429 mg, 2.25 mmol) were mixed in ethanol (35 mL) and heated at 70 °C overnight. After evaporation to dryness, the crude product was purified by column chromatography on silica gel (eluent: dichloromethane-methanol 10:1 v/v). Yellow solid, 195 mg (90 %). ^{1}H NMR (DMSO-d_6) δ 3.80 (s, 3H), 6.70 (d, J = 7.3 Hz, 2H), 6.87 (t, J = 8.1 Hz, 1H), 7.12 (m, 3H), 7.21 (t, J = 8.0 Hz, 2H), 7.56 (dd, J = 8.2, 1.4 Hz, 1H), 10.66 (bs, 1H). ^{13}C NMR (DMSO-d_6) δ 55.8, 112.5, 115.2, 117.0, 117.5, 119.4, 121.0, 128.5, 134.8, 139.2, 148.9, 152.1, 155.0. LRMS (ESI$^+$): *m/z* calcd. for $C_{18}H_{14}N_2O_2$ $[M + H]^+$ 291.1; found 291.2

Perimidine **2** (2-(6-methyl-2-pyridyl)-1*H*-perimidine)

Naphthalene-1,8-diamine (119 mg; 0.75 mmol), 3-methylpyridine-2-carbaldehyde (91 mg; 0.75 mmol) and sodium pyrosulfite (429 mg, 2.25 mmol) were mixed in ethanol (35 mL) and heated at 70 °C overnight. After evaporation to dryness, crude product was purified by column chromatography on silica gel (eluent: diethyl ether). Brick-red solid, 153 mg (79 %). ^{1}H NMR (DMSO-d_6) δ 2.64 (s, 3H), 6.70 (dd, J = 7.3, 1.0 Hz, 1H), 6.78 (dd, J = 7.4, 1.0 Hz, 1H), 7.02 (m, 1H), 7.08 (m, 1H), 7.12 (t, J = 7.9 Hz, 1H), 7.19 (t, J = 7.8 Hz, 1H), 7.47 (dd, J = 7.6, 0.9 Hz, 1H), 7.88 (t, J = 7.8 Hz, 1H), 8.09 (dt, J = 7.8, 0.9 Hz, 1H), 10.61 (bs, 1H). ^{13}C NMR (DMSO-d_6) δ 23.9, 103.4, 114.1, 117.8, 118.7, 119.7, 125.5, 128.1, 128.5, 128.8, 135.1, 137.5, 137.9, 144.9, 148.7, 150.8, 157.2. LRMS (ESI$^+$): *m/z* calcd. for $C_{17}H_{13}N_3$ $[M + H]^+$ 260.1; found 260.0.

3.3. Docking to TET1 and TET2 proteins

At the present time no high-resolution 3D structure of the catalytic domain of human TET1 has been deposited in the PDB database. Three entries for high-resolution structures of the iron-containing catalytic domain of human TET2 are available (PDB ids 4NM6, 5D9Y and 5DEU, L. Hu et al., 2013; L. Hu et al., 2015) [29,38,53]. To overcome this limitation, Chua et al. constructed a 3D structural model of human TET1 based on the crystal structure of human TET2 (PDB ID: 4NM6), with computational methods described in the Supplementary Data section of their publication. Their approach was followed to generate model of the catalytic domain of TET1. Non-essential ligands, double conformations, solvent molecules, and water molecules were removed from the proteins using ChimeraX [54]. For the addition of the missing stretch of 5 amino acids, we used the corresponding segment in the AlphaFold model of TET1 (AF ID Q8NFU7) [55]. A large stretch of missing residues (ca. 480 amino-acids) was modelled using an artificial polyGLY(8) stretch. Model superposition operations were performed using the ccp4MG program [56]. An additional step of CHARMM model equilibration protocol made the model slightly different from the initial TET2 structure (PDB id 4NM6) [57]. The energy-optimized 3D model was subsequently utilized for docking calculations, which were carried out using AutoDock Vina [58]. The molecular model of TET2 was generated from the 1.8 Å resolution crystal structure of TET2 (PDB id 5DEU) [41]. Further modelling was performed as for TET1. For the visualizations of models, we used both Coot and ChimeraX [40,54].

The search was performed within a box measuring 20 × 20 × 20 Å, centred at the entrance of the active site and positioned near the Fe(II) ion.

Molecular docking on the TET1 and TET2 models was performed both before and after CHARMM model equilibration [57]. Molecular docking simulations were carried out using AutoDock Vina [58,59]. ChemDraw was used to prepare chemical structure of the inhibitors for docking, and the structural preparation similar to that of the proteins was carried out according to the AutoDock Vina software manual [58].

3.4. Iron binding affinity of the prepared chelators

The interaction between chelators and Fe(II) ions was investigated using UV–Vis spectroscopy in an aqueous solution (water/DMSO, 99:1, v/v). Since the solvent significantly affects binding constants, all titrations were conducted under identical conditions while maintaining a constant DMSO to water ratio. Conditional constants (Ks) were derived from the absorbance changes (ΔA) of the chelators at the spectral maximum of their complexes with Fe(II), employing nonlinear regression analysis with Letagrop Spefo 2005 software. A comprehensive description of the computational model was made by Selen et al. [60] The concentration of the chelators was fixed at 10 μM, while the concentrations of Fe(II) varied from 0 to 0.5 mM, employing the same methodology as in the investigation of the interactions of organic hosts and metal ions in an aqueous media [33,37,61]. The solutions were continuously mixed in the cuvette throughout the titration process and after each addition of Fe(II) ion.

3.5. TET1 and TET2 inhibition assay

The procedure was adapted from the manual (Bioscience; TET1: 50651, TET2: 50652). First, TBST buffer (1X TBS, pH 8.0, containing 0.05 % Tween-20) was prepared. Next, 4.0X TET Assay Buffer (TAB) was diluted to 1.5X TAB and 1.0X TAB, ensuring uniformity with distilled water. The TET enzyme from the kit was thawed and diluted to 5.0 ng/μL for TET1 and 10 ng/μL for TET2 using 1.0X TAB. The primary antibody was diluted 100-fold with blocking buffer, while the secondary antibody was diluted 1000-fold with the same blocking buffer. The DMSO inhibitor solutions were diluted with 1.0X TAB to the desired concentration, ensuring that the solutions contained 5 % DMSO. The concentrations of the tested inhibitors included 0.1, 0.5, 1, 5, 10, and 50 μM, with each concentration replicated four times. In both kits, a concentration of 0.12 mM of Fe(II) ion was utilized. For the TET2 kit, the concentration was augmented by the addition of $Fe(NH_4)_2(SO_4)_2$. In the provided 96-well plate, 200 μL of TBST buffer was added to each well and incubated at room temperature for 15 min. After incubation, TBST buffer was removed, and 20 μL of 1.5X TAB, 10 μL of the inhibitor solution, and 20 μL of diluted TET enzyme were added to each well. For control wells, 10 μL of a 5 % DMSO solution and 20 μL of 1.0X TAB were added. The mixture was incubated at room temperature for 2 h. The reaction solution was then removed, and each well was washed three times with TBST buffer (200 μL, 200 μL, and 100 μL). Next, 100 μL of blocking buffer and 53 μL of the diluted primary antibody were added,

and the mixture was shaken gently at room temperature for 1 hour. After completing this step, the diluted primary antibody was removed, and the wells were washed three times with TBST buffer (200 µL, 200 µL, and 100 µL). Then, 100 µL of blocking buffer was added to each well, and the mixture was shaken at room temperature for an additional 10 min before the blocking buffer was discarded. The diluted secondary antibody was added, and the mixture was shaken at room temperature for 30 min. Once this step was complete, the diluted secondary antibody was removed, and the wells were washed three times with TBST buffer (200 µL, 200 µL, and 100 µL). Finally, 100 µL of blocking buffer was added to each well, and the mixture was shaken at room temperature for 10 min before the blocking buffer was removed. Substrate A for horseradish peroxidase (HRP) and substrate B for HRP were mixed in a 1:1 ratio, and 100 µL of the HRP solution was added to each well. Immediately afterwards, the chemiluminescence was read using the Spark (Tecan) plate reader.

4. Conclusion

Perimidines **1** and **2** (substituted by 2-hydroxyphenyl and 2-pyridyl groups, respectively) were synthesised and characterised using spectroscopic techniques such as ESI-MS, 1H NMR, and 13C NMR spectroscopy. Lastly, they were studied for their ability to chelate Fe(II) ions and for in vitro inhibitory activity against TET1 and TET2. Both perimidines **1** and especially **2** exhibited excellent inhibitory activity and selectivity for TET1. For example, perimidine **2** displayed more than ten times lower IC_{50} values for the TET1 protein compared to TET2 (1.02 vs. 13.5 µM, respectively). Through molecular docking, we identified that perimidines **1** and **2** block the iron coordination groups (HIS 1382 and ASP 1384) and ARG 1261 (binding deoxyribose and α-ketoglutarate) in TET1/2 proteins. Results from analytical and *in silico* studies indicate that perimidines **1** and **2** can also bind to the catalytic Fe(II) ion in the active site. In future research, we plan to focus on optimising the structural properties of perimidine inhibitors to better understand their inhibitory mechanisms and conduct biological studies of TET protein inhibitors.

Funding

This work was supported by projects of Charles University in Prague [SVV260637; UNCE 204091; Progres LF1 Q38 and Q27, Cooperatio Carles University]; the Ministry of Education, Youth, and Sports grants no. LM2023053 (EATRIS-CZ). The work on this paper was supported by the Czech Science Foundation grant GA25-15918S; and by MULTI-OMICS_CZ (Programme Johannes Amos Comenius, Ministry of Education, Youth and Sports of the Czech Republic, ID Project CZ.02.01.01/00/23_020/0008540) co-funded by the European Union. The study was also supported by the Ministry of Healthy, Czech Republic grant no. RVO-VFN 64165. We are also grateful for the support from the project National Institute for Cancer Research (Programme EXCELES, ID Project No. LX22NPO5102 and LX22NPO5107), funded by the European Union, Next Generation EU. The project "Center for Tumor Ecology - Research of the Cancer Microenvironment Supporting Cancer Growth and Spread" (reg. No. CZ.02.1.01/0.0/0.0/16_019/0000785) is supported by the Operational Programme Research, Development and Education.

CRediT authorship contribution statement

Zdeněk Kejík: Writing – review & editing, Writing – original draft, Formal analysis. **Robert Kaplánek:** Writing – review & editing, Formal analysis, Data curation. **Nikita Abramenko:** Formal analysis, Data curation. **Frédéric Vellieux:** Methodology, Formal analysis. **Kateřina Veselá:** Writing – original draft, Methodology, Investigation, Data curation. **Petr Babula:** Supervision, Formal analysis. **Michal Masařík:** Writing – review & editing, Supervision. **Jan Ulrich:** Investigation, Formal analysis, Data curation. **Kateřina Kučnirová:** Investigation, Data curation. **Jan Hajduch:** Writing – review & editing, Supervision, Formal analysis. **Pavel Martásek:** Supervision, Methodology, Formal analysis, Conceptualization. **Milan Jakubek:** Writing – review & editing, Writing – original draft, Supervision, Resources, Project administration, Funding acquisition, Formal analysis, Conceptualization.

Declaration of competing interest

The authors declare that they have no known competing financial interests or personal relationships that could have appeared to influence the work reported in this paper.

Acknowledgment

We are very grateful to Dr. Božena Hosnedlová for her kind assistance and guidance in the study of chelators properties.

Supplementary materials

Supplementary material associated with this article can be found, in the online version, at doi:10.1016/j.molstruc.2025.143720.

Data availability

Data will be made available on request.

References

[1] A. Yilmaz, E. Grotewold, Components and mechanisms of regulation of gene expression, Methods Mol. Biol. 674 (2010) 23–32.
[2] H.M. Abdolmaleky, et al., Epigenetics in evolution and adaptation to environmental challenges: pathways for disease prevention and treatment, Epigenomics. (2025) 1–17.
[3] A. Nishiyama, M. Nakanishi, Navigating the DNA methylation landscape of cancer, Trends in Genetics 37 (11) (2021) 1012–1027.
[4] D.Q. Shi, et al., New insights into 5hmC DNA modification: generation, distribution and function, Front. Genet. 8 (JUL) (2017).
[5] Z.D. Smith, A. Meissner, DNA methylation: roles in mammalian development, Nature Reviews Genetics 14 (3) (2013) 204–220.
[6] J. Xie, et al., Dynamic regulation of DNA methylation and brain functions, Biology. (Basel) 12 (2) (2023).
[7] K. Joshi, et al., Mechanisms that regulate the activities of TET proteins, Cell Mol. Life Sci. 79 (7) (2022) 363.
[8] P. Melamed, et al., Tet enzymes, variants, and differential effects on function, Front. Cell Dev. Biol. (2018) 6.
[9] H. Huang, et al., TET1 plays an essential oncogenic role in MLL-rearranged leukemia, Proc. Natl. Acad. Sci. u S. a 110 (29) (2013) 11994–11999.
[10] C.R. Good, et al., TET1-Mediated hypomethylation activates oncogenic signaling in triple-negative breast cancer, Cancer Res. 78 (15) (2018) 4126–4137.
[11] P.T. Filipczak, et al., p53-Suppressed oncogene TET1 prevents cellular aging in lung cancer, Cancer Res. 79 (8) (2019) 1758–1768.
[12] M. Ko, et al., Impaired hydroxylation of 5-methylcytosine in myeloid cancers with mutant TET2, Nature 468 (7325) (2010) 839–843.
[13] Y. Guan, et al., A therapeutic strategy for preferential targeting of TET2 mutant and TET-dioxygenase deficient cells in myeloid neoplasms, Blood Cancer Discov. 2 (2) (2021) 146–161.
[14] A.K. Singh, et al., Selective targeting of TET catalytic domain promotes somatic cell reprogramming, Proc. Natl. Acad. Sci. u S. a 117 (7) (2020) 3621–3626.
[15] D. Bellavia, et al., The binomial "inflammation-epigenetics" in breast cancer progression and bone metastasis: iL-1β actions are influenced by TET inhibitor in MCF-7 cell line, Int. J. Mol. Sci. (23) (2022) 23.
[16] D. Liu, G. Li, Y. Zuo, Function determinants of TET proteins: the arrangements of sequence motifs with specific codes, Brief. Bioinformatics 20 (5) (2019) 1826–1835.
[17] K. Šimelis, et al., Selective targeting of human TET1 by cyclic peptide inhibitors: insights from biochemical profiling, Bioorg. Med. Chem. 99 (2024) 117597.
[18] K. Nishio, et al., Thioether macrocyclic peptides selected against TET1 compact catalytic domain inhibit TET1 catalytic activity, Chembiochem. 19 (9) (2018) 979–985.
[19] D. Cirillo, F. Pentimalli, A. Giordano, Peptides or small molecules? Different approaches to develop more effective CDK inhibitors, Curr. Med. Chem. 18 (19) (2011) 2854–2866.
[20] S. Dasgupta, et al., Designing of novel zinc(ii) Schiff base complexes having acyl hydrazone linkage: study of phosphatase and anti-cancer activities, Dalton Transactions 49 (4) (2020) 1232–1240.

[21] A. Shakoor, et al., Synthesis of novel benzimidazole analogs for neurodegenerative diseases by targeting prolyl oligopeptidase, ChemistrySelect. 9 (34) (2024) e202401904.
[22] H. Ullah, et al., Exploring the anti-diabetic potential of bis-schiff base derivatives of benzimidazole: in-vitro α-amylase, α-glucosidase inhibition, molecular docking, ADMET and DFT studies, Comput. Biol. Chem. 118 (2025) 108497.
[23] A. Shakoor, et al., *Novel benzimidazole derivatives as effective inhibitors of prolyl oligopeptidase: synthesis,* in vitro *and in silico analysis*, Future Med. Chem. 16 (1) (2024) 43–58.
[24] Hamidullah, et al., *Novel benzimidazole-based azine derivatives as potent urease inhibitors: synthesis,* in vitro *and in silico approach*, Future Med. Chem. 16 (22) (2024) 2337–2350.
[25] A. Shakoor, et al., Synthesis of benzimidazole-based hydrazones as potential anticarbonic anhydrase agents: a theoretical and experimental investigations, Zeitschrift für Naturforschung C (2025).
[26] A. Srovnalová, et al., Synthesis and evaluation of cyclobut-3-ene-1,2-dione-3-hydrazones with benzothiazole moiety as novel anticancer agents inducing nonapoptotic oncosis-like cell death, Biomedicine & Pharmacotherapy 190 (2025) 118404.
[27] R. Kaplánek, et al., TET protein inhibitors: potential and limitations, Biomed. PharmacOther 166 (2023) 115324.
[28] V. Antonyová, et al., Non-psychotropic cannabinoids as inhibitors of TET1 protein, Bioorg. Chem. 124 (2022) 105793.
[29] V. Antonyová, et al., Targeting of the mitochondrial TET1 protein by pyrrolo[3,2-b]pyrrole chelators, Int. J. Mol. Sci. 23 (18) (2022) 10850.
[30] Y. Guan, et al., Eltrombopag inhibits TET dioxygenase to contribute to hematopoietic stem cell expansion in aplastic anemia, J. Clin. Invest. 132 (4) (2022).
[31] N. Harry, et al., A comprehensive overview of perimidines: synthesis, chemical transformations and applications, Curr. Org. Chem. (2020) 24.
[32] D. Roy, A. Chakraborty, R. Ghosh, Perimidine based selective colorimetric and fluorescent turn-off chemosensor of aqueous Cu2+: studies on its antioxidant property along with its interaction with calf thymus-DNA, RSC. Adv. 7 (64) (2017) 40563–40570.
[33] M. Jakubek, et al., Perimidine-based synthetic receptors for determination of copper(II) in water solution, Supramol. Chem. 30 (3) (2018) 218–226.
[34] G. Park, et al., Novel iron complexes and chelators based on cis,cis-1,3,5-triaminocyclohexane: iron-mediated ligand oxidation and biochemical properties, JBIC Journal of Biological Inorganic Chemistry 3 (5) (1998) 449–457.
[35] M.T. Stauffer, L.J. Hunter, S.K. Troncone, Determination of iron in abandoned mine drainage by UV-vis spectrophotometry and flame atomic absorption spectrophotometry, Spectroscopy Letters 40 (3) (2007) 429–437.
[36] D.C. Zhou, et al., Design, synthesis and biological evaluation of novel perimidine o-quinone derivatives as non-intercalative topoisomerase II catalytic inhibitors, Bioorg. Chem. 91 (2019) 103131.
[37] M. Jakubek, et al., Hydrazones as novel epigenetic modulators: correlation between TET 1 protein inhibition activity and their iron(II) binding ability, Bioorg. Chem. 88 (2019) 102809.
[38] L. Hu, et al., Crystal structure of TET2-DNA complex: insight into TET-mediated 5mC oxidation, Cell 155 (7) (2013) 1545–1555.
[39] G.N.L. Chua, et al., Cytosine-based TET enzyme inhibitors, ACS. Med. Chem. Lett. 10 (2) (2019) 180–185.
[40] P. Emsley, et al., Features and development of Coot, Acta Crystallogr. D. Biol. Crystallogr. 66 (Pt 4) (2010) 486–501.
[41] H.M. Berman, et al., The protein data bank, Nucleic. Acids. Res. 28 (1) (2000) 235–242.
[42] D.T. Infield, et al., Cation-π interactions and their functional roles in membrane proteins, J. Mol. Biol. 433 (17) (2021) 167035.
[43] E.G. Kovaleva, J.D. Lipscomb, Versatility of biological non-heme Fe(II) centers in oxygen activation reactions, Nat. Chem. Biol. 4 (3) (2008) 186–193.
[44] C.G. Yeh, et al., Second coordination sphere effects on the mechanistic pathways for dioxygen activation by a ferritin: involvement of a tyr radical and the identification of a cation binding site, Chembiochem. 23 (13) (2022) e202200257.
[45] A.P. Tauer, Theoretical Investigations of PI-PI and Sulfur-PI Interactions and their Roles in Biomolecluar Systems, Georgia Institute of Technology, 2005.
[46] R. Calinsky, Y. Levy, Histidine in proteins: pH-dependent interplay between π–π, cation–π, and CH–π interactions, J. Chem. Theory. Comput. 20 (15) (2024) 6930–6945.
[47] B.L. Schottel, H.T. Chifotides, K.R. Dunbar, Anion-pi interactions, Chem. Soc. Rev. 37 (1) (2008) 68–83.
[48] M.O. Sinnokrot, C.D. Sherrill, Substituent effects in π−π interactions: sandwich and T-shaped configurations, J. Am. Chem. Soc. 126 (24) (2004) 7690–7697.
[49] D. Bellotti, M. Remelli, Deferoxamine B: a natural, excellent and versatile metal chelator, Molecules. 26 (11) (2021).
[50] Y.-C. Chen, *Beware of docking*!, Trends. Pharmacol. Sci. 36 (2) (2015) 78–95.
[51] S. Palei, et al., A high-throughput effector screen identifies a novel small molecule scaffold for inhibition of ten-eleven translocation dioxygenase 2, RSC. Med. Chem. 13 (12) (2022) 1540–1548.
[52] D. Bellavia, et al., The binomial "inflammation-epigenetics" in breast cancer progression and bone metastasis: IL-1β actions are influenced by TET inhibitor in MCF-7 cell line, Int. J. Mol. Sci. 23 (23) (2022) 15422.
[53] L. Hu, et al., Structural insight into substrate preference for TET-mediated oxidation, Nature 527 (7576) (2015) 118–122.
[54] E.C. Meng, et al., UCSF ChimeraX: tools for structure building and analysis, Protein Science 32 (11) (2023) e4792.
[55] M. Varadi, et al., AlphaFold protein structure database in 2024: providing structure coverage for over 214 million protein sequences, Nucleic. Acids. Res. 52 (D1) (2023) D368–D375.
[56] S. McNicholas, et al., Presenting your structures: the CCP4mg molecular-graphics software, Acta Crystallographica Section D 67 (4) (2011) 386–394.
[57] S. Jo, et al., CHARMM-GUI: a web-based graphical user interface for CHARMM, J. Comput. Chem. 29 (11) (2008) 1859–1865.
[58] O. Trott, A.J. Olson, AutoDock Vina: improving the speed and accuracy of docking with a new scoring function, efficient optimization, and multithreading, J. Comput. Chem. 31 (2) (2010) 455–461.
[59] J. Eberhardt, et al., AutoDock Vina 1.2.0: new docking methods, expanded force field, and Python bindings, J. Chem. Inf. Model. 61 (8) (2021) 3891–3898.
[60] L.G. Sillen, High-speed computers as supplement to graphical methods .3. Twist matrix methods for minimizing error-square sum in problems with many unknown constants, Acta Chem. Scand. 18 (5) (1964), p. 1085-&.
[61] M. Jakubek, et al., Water soluble chromone Schiff base derivatives as fluorescence receptor for aluminium(III), Supramol. Chem. 29 (1) (2017) 1–7.